ISBN: 978-3-95450-222-6 ISSN: 2673-5350 doi:10.18429/JACoW-IBIC2020-THPP11

STUDY OF MULTI-BLADED PHOTON BPM DESIGNS

Y.-R. E. Tan*, AS - ANSTO, Clayton, Australia

Abstract

New beamlines will be installed in at the AS in the next few years and photon BPMs will be part of the front end design. A theoretical study of the potential benefits of a multi-bladed photon BPM design has been simulated using beam profiles from SPECTRA. The results show that it is possible to remove the gap/field dependence of the photon BPM by a least squares fit of the distribution, in this test case a Gaussian distribution, to the beam profile sampled by the multiple blades.

INTRODUCTION

The majority of photon BPMs (XBPMs) that are located in the front-end of beamlines at light sources use metallic blades as the detector. As synchrotron radiation illuminate the surface of the metallic blades, photo-electrons are ejected (PE effect) and the current is proportional to the photon flux and energy. The drain current at the blade is measured using a picoammeter or equivalent. The strength of such a design is its fairly straight forward design, ability to reach µm resolutions and robustness. The most typical configuration is a pair of blades on either side of the photon beam to measure the vertical displacement. This is typical for dipole and wiggler sources. If transverse directions are required then four blades are used, either arranged in the cardinal directions or rotated by 45°. This is commonly used for undulator sources. There are two well known issues, upstream contamination from other radiation sources and a gain (calibration factor) that depends on the photon distribution, which in turn depends on the insertion device parameter, K_u. This is particularly problematic for APPLEII type insertion devices that have many more degrees of freedom and potential photon distributions. To overcome some of the deficiencies issue other approaches to photon beam detection is being developed such as photoconduction based designs using diamond or SiC based detectors [1], fluorescence based [2] or residual gas [3].

The first issue of upstream photon contamination is difficult to address and is only an issue if the photon flux from the ID at the blade is comparable to the flux from other sources (blades are too far away or K < 1) [4]. This report investigates the potential benefits of fitting a Gaussian distribution to the photon distribution sampled at four or more locations. This approach is investigated numerically and compared to traditional methods to show that it has the potential to be more robust against changes to K_u.

* eugene.tan@ansto.gov.au

PHOTON DISTRIBUTION AND BLADE CONFIGURATION

The source radiation will be modelled on a 22 mm period IVU with a K_u between 1.03 and 1.85. Some design parameters include an assumed beamline acceptance of 1.11 mrad by 0.40 mrad and XBPM's located 6.9 m from the source. Assuming the extent of the blade is located at +0.3 mrad and maximum beam offsets of ± 1 mm, the minimum observation angle of the blade is approximately 0.2 mrad. In Fig. 1 the energy spectrum at two extreme K_u values has been calculated using SPECTRA [5] showing that above 3 keV the flux peaks have decreased by an order of magnitude. For this study we have limited simulation to an integration of photon distributions calculated at 100 intervals between 100 eV and 3.5 keV. A plot of such a distribution is shown in Fig. 2 for $K_u = 1.03$ along with the blade configuration. A simple blade geometry has been adopted, with a set of 2 mm long vertical blades with a range of horizontal gaps between the blades, $S_x = [0.5, 1.0, 1.5, 2.0, 2.5]$ (mm).

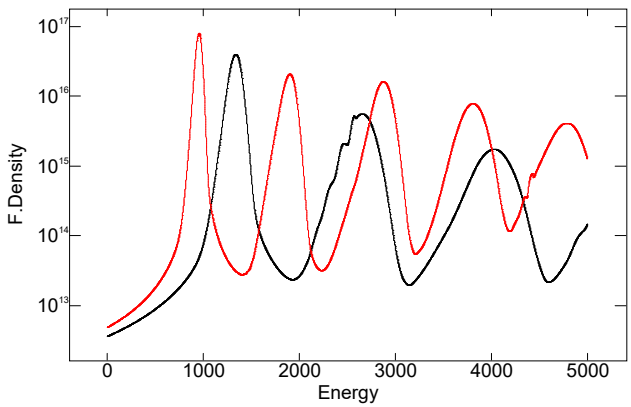

Figure 1: Flux density at an observation angle $\theta_y = 0.2$ mrad for a $K_u = 1.03$ (black) and 1.85 (red).

CENTROID CALCULATIONS

Four methods will be evaluated. The first two are the difference over sum (DS) method given by

$$x^{DS} = K_x^{DS}\frac{[(b_4 + b_9) - (b_2 + b_7)]}{b_2 + b_4 + b_7 + b_9}$$

$$y^{DS} = K_y^{DS}\frac{[(b_2 + b_4) - (b_9 + b_7)]}{b_2 + b_4 + b_7 + b_9}$$

the center of mass (CM) method,

$$x^{CM} = K_x^{CM}\frac{\Sigma_{n=1}^{5} w_n b_n}{\Sigma_{n=1}^{5} b_n}$$

$$y^{CM} = K_y^{CM}\frac{\Sigma_{n=12,9,4,11} w_n b_n}{\Sigma_{n=12,9,4,11} b_n}$$

ISBN: 978-3-95450-222-6 ISSN: 2673-5350 doi:10.18429/JACoW-IBIC2020-THPP11

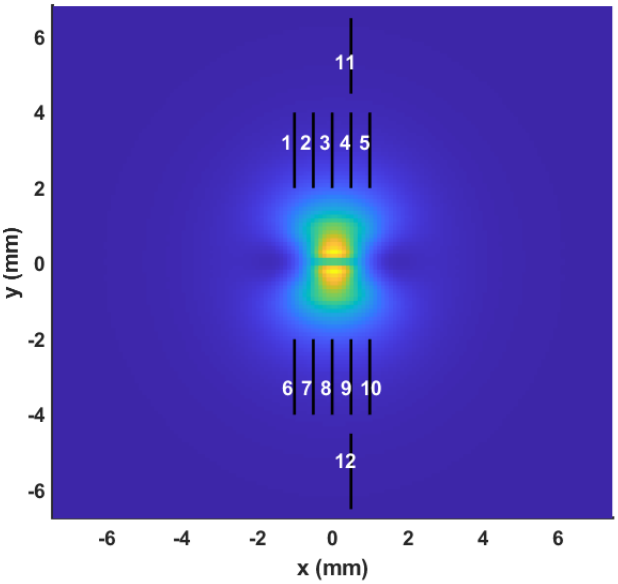

Figure 2: Photon distribution for $K_u = 1.03$. In this plot the vertical blade arrangement has a horizontal gap between the blades of $S_x = 0.5$ mm. In the simulations, five different configuration of $S_x = [0.5, 1.0, 1.5, 2.0, 2.5]$ will be compared. Blades, b_3 and b_8 remain in the same location while all the others are shifted.

where $K_{x,y}$ are the scaling/calibration factors and b_n are signals from the individual blades shown in Fig. 2. The final two are Gaussian fitting algorithms: Caruana's algorithm and Guo's improved iterative version found in Reference [6]. Guo's algorithm improves on Caruana's by applying a weighted least squares technique, making it more immune to the effects of noise in the data.

SIMULATION

The photon distribution is shifted horizontally and vertically over a range of ±1 mm and the signals from the blade is the integration of the photon flux along the length of the blade[1]. The peak of the photon distribution is normalised to unity and noise with a sigma of 0.005 was introduced to each of the blades to test the response of the methods in the presence of noise. For each offset, 100 data sets with noise was generated. The values of $K_{x,y}$ is given by the gradient a line over the small range $x/y = [-0.2\text{ mm}, +0.2\text{ mm}]$.

K_u Dependence

With the effective values of $K_{x,y}$ for the different blade separations and undulator parameters, it is possible to get a sense of how the four methods compare. Figure 3 shows just one example of the relative change in the gain, $\delta K_{x,y}$, as a function of K_u for $S_x = 1$ mm. In this particular configuration the Gaussian methods are decidedly less affected

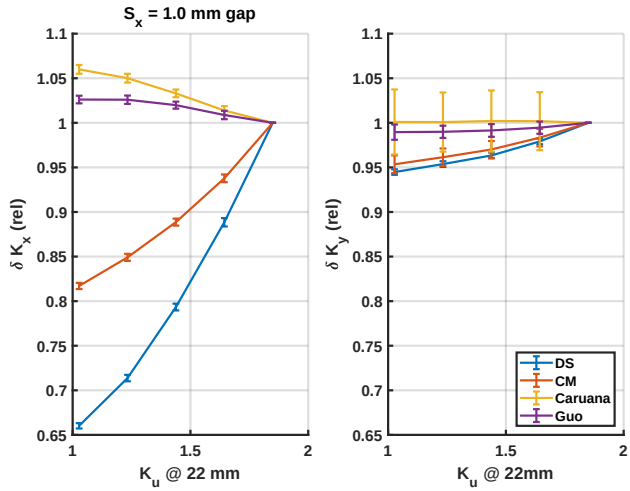

Figure 3: Relative change in $K_{x,y}$ as a function of K_u

Table 1: Table of $G_{x,y} = \Delta\delta K_{x,y}/\Delta K_u$. The Group of Values at the Top Represent G_x and the Bottom Group G_y. The Coloured Boxes Represent the Configurations Where the Noise in the Position Resolution is Less Than 15 µm as Shown in Table 2

S_x	DS	CM	Caruana	Guo
0.5 mm	0.469	0.408	0.001	-0.003
1.0 mm	0.416	0.221	-0.076	-0.034
1.5 mm	0.320	0.086	-0.108	-0.002
2.0 mm	0.222	0.017	-0.075	-0.148
2.5 mm	0.140	-0.068	-0.056	-0.238
3.0 mm	0.055			
4.0 mm	-0.001			
5.0 mm	-0.009			
0.5mm	0.127	0.104	0.000	0.029
1.0mm	0.066	0.056	0.001	0.011
1.5mm	-0.024	-0.010	-0.002	-0.016
2.0mm	-0.105	-0.066	-0.001	-0.038
2.5mm	-0.159	-0.098	0.005	-0.045
3.0mm	-0.177			
4.0mm	-0.151			
5.0mm	-0.099			

by the change in K_u. To see how this changes for different values of S_x, the gradient of the the relative change given by $G_{x,y} = \Delta\delta K_{x,y}/\Delta K_u$ has been calculated and tabulated in Table 1.

In the case of DS, for a given vertical gap (required stay clear for the beam line acceptance) and this particular geometry, it is not possible to simultaneously minimise G_x ($S_x = 4.0$ mm) and G_y ($S_x = 1.4$ mm). The same is true for the CM method and shows very similar trends to the DS method. This is to be expected as both methods perform linear extrapolation and would only be accurate if the photon distribution resembled a triangle, or where the gradients,

[1] The photoemission properties of the material of the blade are not considered as this study is a comparison of algorithms

ISBN: 978-3-95450-222-6 ISSN: 2673-5350 doi:10.18429/JACoW-IBIC2020-THPP11

Table 2: Minimum and Maximum Linearity Range (in mm) and the Minimum and Maximum Position Resolution, $\sigma_{x,y}$ (in µm), for the Range of $K_u = [1.03, 1.85]$. The Highlighted Boxes Indicate Where $\sigma_{x,y} < 15$ µm

S_x	DS (mm / µm)	CM (mm / µm)	Caruana (mm / µm)	Guo (mm / µm)
0.5mm	0.63-0.80 / 12.6-19.3	0.53-0.80 / 09.1-13.2	0.50-0.80 / 15.6-21.7	0.51-0.80 / 15.0-21.5
1.0mm	0.47-0.61 / 07.5-10.5	0.60-0.67 / 08.7-09.5	0.48-0.59 / 09.9-10.7	0.61-0.74 / 08.4-10.1
1.5mm	0.46-0.52 / 07.3-08.5	0.76-0.80 / 11.3-12.1	0.57-0.62 / 13.0-15.6	0.80-0.80 / 09.1-09.8
2.0mm	0.48-0.50 / 08.5-08.7	0.80-0.80 / 15.5-17.8	0.70-0.78 / 22.8-29.6	0.50-0.80 / 11.0-11.6
2.5mm	0.49-0.51 / 09.9-11.5	0.80-0.80 / 21.6-26.2	0.80-0.80 / 41.9-55.2	0.55-0.60 / 13.3-15.5
3.0mm	0.51-0.57 / 12.6-16.2			
4.0mm	0.66-0.72 / 23.6-33.0			
5.0mm	0.79-0.80 / 45.8-63.1			
0.5mm	0.41-0.42 / 05.8-06.2	0.46-0.48 / 16.2-17.7	0.80-0.80 / 56.4-74.4	0.39-0.40 / 11.4-13.8
1.0mm	0.42-0.44 / 06.6-08.1	0.48-0.51 / 18.4-22.9	0.80-0.80 / 60.3-82.7	0.40-0.41 / 12.7-16.3
1.5mm	0.44-0.48 / 08.5-12.4	0.53-0.60 / 23.1-33.4	0.80-0.80 / 67.9-99.2	0.41-0.44 / 15.2-22.0
2.0mm	0.50-0.55 / 12.1-20.0	0.60-0.72 / 31.8-51.5	0.80-0.80 / 81.7-123	0.44-0.49 / 20.2-32.4
2.5mm	0.50-0.65 / 18.2-33.1	0.70-0.80 / 46.4-78.4	0.80-0.80 / 102-156	0.48-0.60 / 28.5-49.7
3.0mm	0.63-0.80 / 29.3-55.2			
4.0mm	0.80-0.80 / 74.6-140			
5.0mm	0.80-0.80 / 179-317			

$\Delta b_n / \Delta x$, are similar at the blades and the distribution is symmetric.

As the photon distribution is closer to a Gaussian distribution, using fitting algorithms to extract the sigma, amplitude and offset should be more robust. This is reflected in the results where both Gaussian methods have the smallest values of $G_{x,y}$. The smallest values are achieved when the distribution is sufficiently sampled with closely spaced blades. $G_{x,y}$ increases with increasing values of S_x.

Linearity and Resolution

In addition to minimising the dependence on K_u it is also important to determine the extent of the linear region and the position resolution for a given amount of noise introduced into the system [2]. The linearity range is given as the horizontal or vertical region where the residual error is less than the position resolution. An example of such an analysis of the linearity and resolution is show in Fig. 4 and results of the four methods has been tabulated in Table 2.

In terms of position resolution, the DS method is the best followed by Guo's algorithm. It was surprising to see how sensitive to noise Caruana's algorithm turns out to be. Guo's algorithm was far more robust and showed similar linearity and slightly worse resolution compared to the DS method.

Taking both tables into consideration the CM and Caruana methods would be discarded in favour of the DS and Guo's methods. One issue with the DS method is that to get good linearity and small values for $G_{x,y}$ the blades have to be far apart. This results in smaller signals and therefore poorer position resolution overall. Guo's method on the other hand performs better with blades closer to the centroid, larger

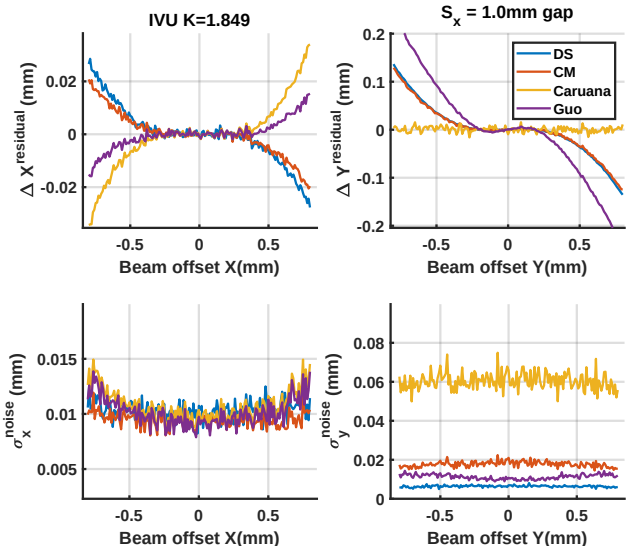

Figure 4: Plot of the residual error (top row) and the spread of the position calculations due to noise on the blades, position resolution (bottom row).

signals and good position resolution overall. In the two cases, optimised configuration and parameters would be:

- DS method: S_x = 1.4 mm, G_x = +0.30, G_y = -0.01, $\sigma_{x,y} \approx 10$ µm, Linear range > ±0.44 mm
- Guo's method: S_x = 1.0 mm, G_x = -0.03, G_y = +0.01, $\sigma_{x,y} \approx 16$ µm, Linear range > ±0.40 mm

This shows that using more blades and a Gaussian fitting algorithm can be a viable option that minimise both G_x and G_y the dependence on K_u. What has not been considered here are mechanical considerations such as shadowing of

[2] The resolution calculation is used here as a measure of robustness of the four methods to noise

ISBN: 978-3-95450-222-6 ISSN: 2673-5350 doi:10.18429/JACoW-IBIC2020-THPP11

up and downstream XBPMs, material response and thermal considerations (larger signals → higher heat-loads).

CONCLUSION

When using multiple blades and a Gaussian distribution as an approximation of the photon distribution, it is possible to improve XBPMs robustness to changes in K_u while maintaining linearity and resolution. An extension of this would be to adapt Guo's algorithm to fit a 2D Gaussian function and potentially requiring fewer number of blades.

REFERENCES

[1] S. Nida *et al*, "Silicon carbide X-ray beam position monitors for synchrotron applications", *J. Synchrotron Rad.*, vol. 26, pp. 28–35, 2019. doi:10.1107/S1600577518014248

[2] B. X. Yang *et al.*, "Design and Development for the Next Generation X-ray Beam Position Monitor System at the APS", in *Proc. IPAC'15*, Richmond, VA, USA, May 2015, pp. 1175–1177. doi:10.18429/JACoW-IPAC2015-MOPWI014

[3] P. Ilinski, U. Hahn, H. Schulte-Schrepping, and M. Degenhardt, "Residual Gas X-ray Beam Position Monitor Development for PETRA III", *AIP Conference Proceedings*, vol. 879, pp. 782–785, 2007. 10.1063/1.2436177

[4] G. Decker and O. Singh, "Method for reducing x-ray background signals from insertion device x-ray beam position monitors", *Phys. Rev. ST Accel. Beams*, vol. 2, p. 112801, 1999. doi:10.1103/PhysRevSTAB.2.112801

[5] T. Tanaka and H. Kitamura, "SPECTRA: a synchrotron radiation calculation code", *J. Synchrotron Rad.*, vol. 8, pp. 1221–1228, 2001. doi:10.1107/S090904950101425X

[6] H. Guo, "A Simple Algorithm for Fitting a Gaussian Function [DSP Tips and Tricks]", *IEEE Signal Processing Magazine*, vol. 28, pp. 134–137, 2011, doi:10.1109/MSP.2011.941846